



Kent Academic Repository

Rigden, Jane S., Burke, Terry, Newport, Robert J., Wilson, J.I.B., Jubber, M.G., Morrison, N.A. and John, Peter (1996) *Shallow angle X-ray diffraction from As-deposited diamond thin films*. *Journal of the Electrochemical Society*, 143 (3). pp. 1033-1037. ISSN 0013-4651.

Downloaded from

<https://kar.kent.ac.uk/15967/> The University of Kent's Academic Repository KAR

The version of record is available from

<https://doi.org/10.1149/1.1836577>

This document version

UNSPECIFIED

DOI for this version

Licence for this version

UNSPECIFIED

Additional information

Versions of research works

Versions of Record

If this version is the version of record, it is the same as the published version available on the publisher's web site. Cite as the published version.

Author Accepted Manuscripts

If this document is identified as the Author Accepted Manuscript it is the version after peer review but before type setting, copy editing or publisher branding. Cite as Surname, Initial. (Year) 'Title of article'. To be published in *Title of Journal*, Volume and issue numbers [peer-reviewed accepted version]. Available at: DOI or URL (Accessed: date).

Enquiries

If you have questions about this document contact ResearchSupport@kent.ac.uk. Please include the URL of the record in KAR. If you believe that your, or a third party's rights have been compromised through this document please see our [Take Down policy](https://www.kent.ac.uk/guides/kar-the-kent-academic-repository#policies) (available from <https://www.kent.ac.uk/guides/kar-the-kent-academic-repository#policies>).

Acknowledgments

Part of this work has been financially supported by Spanish CICYT under the Project Ref. MAT92-0351.

Manuscript submitted April 27, 1995; revised manuscript received Oct. 16, 1995.

Universitat de Barcelona assisted in meeting the publication costs of this article.

REFERENCES

1. H. A. Waggener, *Bell Syst. Tech. J.*, **49**, 473 (1970).
2. H. Seidel, L. Csepregi, A. Heuberger, and H. Baumgärtel, *This Journal*, **137**, 3626 (1990).
3. N. F. Raley, Y. Sugiyama, and T. Van Duzer, *ibid.*, **131**, 161 (1984).
4. P. L. F. Hemment, *Mater. Res. Soc. Symp. Proc.*, **53**, 207 (1986).
5. A. Söderbärg, *This Journal*, **139**, 561 (1992).
6. A. Romano-Rodríguez, A. El-Hassani, A. Pérez-Rodríguez, J. Samitier, J. R. Morante, J. Esteve, and M. C. Acero, *Mater. Res. Soc. Symp. Proc.*, **308**, 361 (1993).
7. M. C. Acero, J. Esteve, J. Montserrat, J. Bausells, A. Pérez-Rodríguez, A. Romano-Rodríguez, and J. R. Morante, *Sensors Actuators A*, **45**, 219 (1994).
8. J. F. Ziegler, J. P. Biersack, and U. Littmark, *The Stopping and Range of Ions in Solids*, Vol. 1, Pergamon Press, Inc., New York (1985).
9. A. Merlos, M. C. Acero, M. H. Bao, J. Bausells, and J. Esteve, *Sensors Actuators A*, **37-38**, 737 (1993).
10. J. Samitier, S. Martinez, A. El-Hassani, A. Pérez-Rodríguez, and J. R. Morante, *Appl. Surf. Sci.*, **63**, 312 (1993).
11. G. M. Igno, N. Zacchetti, D. Della Sala, and C. Coluzza, *J. Vac. Sci. Technol.*, **A7**, 3048 (1989).
12. H. R. Phillip, *This Journal*, **120**, 295 (1973).
13. R. J. Temkin, *J. Non-Cryst. Solids*, **17**, 215 (1975).
14. P. Bourguet, J. M. Dupart, E. Le Tiran, P. Auvray, A. Guivarc'h, M. Salvi, G. Pelous, and P. Henoc, *J. Appl. Phys.*, **51**, 6169 (1980).
15. J. Petruzzello, T. F. McGee, M. H. Frommer, V. Rumennik, P. A. Walters, and C. J. Chou, *J. Appl. Phys.*, **58**, 4605 (1985).
16. W. Skorupa, K. Wollschläger, U. Kreissig, R. Grötzschel, and H. Bartsch, *Nucl. Instrum. Meth. Phys.*, **B19/20**, 285 (1987).
17. R. Schork, H. Ryssel, in *Proceedings of the 10th International Conference on Ion Implantation Technology*, Catania, Italy, June 1994.
18. H. Seidel, L. Csepregi, A. Heuberger, and H. Baumgärtel, *This Journal*, **137**, 3612 (1990).
19. A. Söderbärg, in *Proceedings of 1st International Symposium on Semiconductor Wafer Bonding: Science, Technology and Applications*, U. Gösele, T. Abe, J. Haisma, and M. A. Schmidt, Editors, PV 92-7, p. 190, The Electrochemical Society Proceedings Series, Pennington, NJ (1992).
20. J. Stoemenos, B. Aspar, and J. Margail, in *Silicon on Insulator Technology and Devices*, S. Cristoloveanu, Editor, PV 94-11, p. 16. The Electrochemical Society Proceedings Series, Pennington, NJ (1994).
21. J. Macía, T. Jawhari, A. Pérez-Rodríguez, and J. R. Morante, *ibid.*, p. 148.
22. L. Calvo-Barrio, A. Pérez-Rodríguez, A. Romano-Rodríguez, J. R. Morante, and J. Montserrat, *Mater. Sci. Technol.*, **11**, 1187 (1995).

Shallow Angle X-Ray Diffraction from As-Deposited Diamond Thin Films

J. S. Rigden,* T. M. Burke, and R. J. Newport*

Physics Laboratory, The University, Canterbury, Kent, CT2 7NR, England

J. I. B. Wilson,^a M. G. Jubber,^a N. A. Morrison,^b and P. John^b

^a*Department of Physics and* ^b*Department of Chemistry, Heriot-Watt University, Edinburgh, EH14 4AS, Scotland*

ABSTRACT

We demonstrate the method of diffraction at shallow angles of incidence, using the intrinsically highly collimated x-ray beam generated by a synchrotron source, through the study of diamond thin films in their as-deposited (*i.e.*, on substrate) state. As the incident angle is decreased, scattering from the diamond film can be isolated as contributions from the substrate are reduced. Diamond films deposited onto both silicon and steel substrates have been examined, evidence of an interfacial region between the film and silicon wafer has been observed, and conventional transmission x-ray diffraction has been used as a complement to the shallow angle results from the films deposited on steel.

Introduction

The refractive index of materials at x-ray wavelengths is less than unity; consequently, at incident angles below a critical value total external reflection occurs. Below this critical angle, α_c , limited penetration of the material is achieved via the evanescent mode, and is exponentially damped: in principle sampling depths of ~10 to ~1000 Å may be achieved. Above α_c , the penetration depth increases rapidly with incident angle, and inversely with the wavelength of the radiation, and is limited by photoelectric absorption. Thus, for a given wavelength, a number of characteristic sampling depths (length scales) may be achieved by varying the incident angle.

An experimental method for exploiting this phenomenon is the shallow angle diffraction technique, designed by Lim and Ortiz¹ and recently developed for disordered thin films by Burke *et al.*^{2,3} The method relies on the ability to use an intrinsically highly collimated, low divergence synchrotron radiation beam at shallow angles of incidence in order to limit the x-ray penetration depth, and thereby to render the substrate "invisible." It is the aim of this paper to demonstrate the potential, and the limitations, of the method within the context of the contemporary interest in chemical vapor deposition (CVD) grown thin films of diamond.

Diamond has been used industrially for many years and has been exploited in capacitors, in the electronics industry, in bearings, and as high precision cutters.⁴ It has a unique combination of hardness and strength, a large dielectric constant, and an extremely low coefficient of

* Electrochemical Society Active Member.

friction. However, bulk diamond cannot be engineered into the many physical configurations required to exploit all these properties, and the recent advances allowing diamond to be grown as a thin film or coating have allowed the material to be used in a whole range of new areas, such as x-ray windows, electronic packaging applications, and friction and wear coatings.⁵ Three diamond films of thickness $\sim 5 \mu\text{m}$ were studied using shallow angle diffraction. Film A was a polycrystalline diamond thin film prepared by chemical vapor deposition onto a polished silicon wafer. Films B and C were both produced by CVD onto a steel disk: film B onto stainless steel, film C onto Invar steel. Two additional identical films were produced of film B and film C so that one film of each type could be removed from the substrate and examined by transmission diffraction. The availability of conventional x-ray diffraction data provides a useful benchmark for the shallow angle results. A description of the CVD process parameters is given in Ref. 6, but for illustrative purposes sample A was prepared using a microwave-assisted method (microwave power $\sim 500 \text{ W}$) with 0.5% methane in hydrogen at $\sim 45 \text{ mbar}$ total pressure and with the substrate held at 1000°C ; the $\{100\}$ Si wafer was mechanically scratched with diamond dust to promote nucleation. Diamond deposition on stainless steel is problematic since there is a tendency to form carbides and an associated catalytic formation of graphitic rather than diamond-like carbon sites; this is due especially to the nickel and cobalt components. One way of overcoming this is to etch out the catalytic components, but this can weaken the surface. An additional problem arises from the rapid diffusion of carbon in steel which leads to a slow buildup of carbon on the surface and delays the formation of diamond nuclei. To overcome this in the context of steels and other biomedical materials we have used the shock tube technique.¹⁰

The Shallow Angle Technique

When electromagnetic radiation is incident at an angle α , upon a material with a critical angle for external reflection α_c , it will be affected in one of four ways: (i) if $\alpha < \alpha_c$, the radiation is totally externally reflected, (ii) if $\alpha = \alpha_c$, the refracted beam propagates parallel to the surface of the sample, (iii) if $\alpha > \alpha_c$, the refracted beam passes into the sample, and the near-surface region will be illuminated to a characteristic penetration depth t as in Fig. 1, (iv) if $\alpha \gg \alpha_c$ the refracted beam penetrates through the sample into the interface layer or substrate.

For a material of density $\rho \text{ g cm}^{-3}$, and an incident wavelength λ in angstroms, α_c (in radians) is given by

$$\alpha_c = 1.6 \times 10^{-3} \rho^{1/2} \lambda \quad [1]$$

For an incident angle $\alpha_i < \alpha_c$, the near-surface region of the material will be illuminated to a depth t at which the electric field vector has fallen to $1/e$, where t is given by

$$t_{\alpha_i < \alpha_c} = \frac{\lambda}{2\pi(\alpha_c^2 - \alpha_i^2)^{1/2}} \quad [2]$$

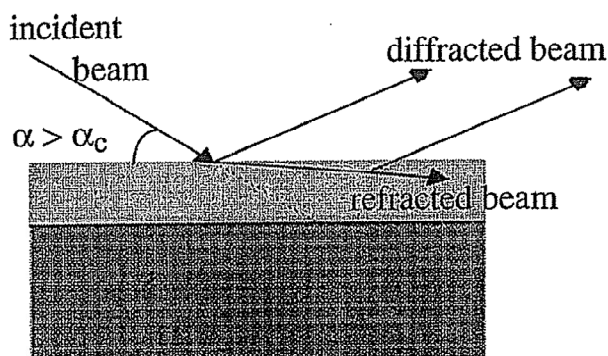


Fig. 1. Geometry for diffraction to occur at shallow angles of incidence.

Above α_c , penetration into the material increases rapidly with the incident angle. If α_i is larger than α_c , but still small, we have⁷

$$t_{\alpha_i > \alpha_c} = \frac{2\alpha_i}{\mu} \quad [3]$$

where μ is the (wavelength dependent) linear attenuation coefficient given by the product of the mass attenuation coefficient and the density.

For example, for a diamond thin film, typically of density 3.52 g cm^{-3} , at an incident x-ray wavelength of 0.5 \AA , $\alpha_c = 1.5 \text{ mrad} = 0.086^\circ$ and $\mu_c = 1.18 \text{ cm}^{-1}$. For a silicon wafer, however, $\mu_{\text{Si}} = 5.57 \text{ cm}^{-1}$; since both the mass attenuation coefficient and density for all steels are high, μ_{steel} is also large; penetration of x-rays into steel at shallow angles is therefore negligible. Table I shows the contrast in penetration depths t for a variety of incident angles α_i , just above α_c , for the diamond film and substrates. The incident angle of 0.05° is just below α_c for diamond at a wavelength of 0.5 \AA , and hence Eq. 2 is used to calculate the penetration depth; t is therefore $1.2 \mu\text{m}$ in this case. However, it is important to note that since problems such as any slight curvature or irregularity in the film (or substrate) surface will result in slight differences in film thickness, it is possible that both the detector (2θ) scan at $\alpha_i = 0.1^\circ$ and at $\alpha_i = 0.05^\circ$ will show contributions to the scattering simultaneously from above and below the critical angle. In addition, we note the obvious point that these films are polycrystalline in nature; however, none of the films have been grown epitaxially and we therefore expect no preferred orientation. Hence, even at the lowest angle of incidence used, where the characteristic probe depth is less than the grain size and overall film thickness (see Fig. 2 and Table I) the diffraction spectrum will be an average over crystalline orientations. The related nature of surface roughness is also of importance at the very lowest angles of incidence; Fig. 2 illustrates the situation with respect to sample A, showing surface roughness to be of order 1 to $2 \mu\text{m}$. It is, therefore, possible that the film's scattering cannot be separated quite as clearly as might be hoped. The much smaller penetration depths for the silicon and steel means that any x-rays which pass through the thin film are quickly absorbed by the substrate.

Experimental

Both the transmission and shallow angle x-ray diffraction data were collected on Station 9.1 at the Synchrotron Radiation Source at Daresbury Laboratory, UK. The intrinsically highly parallel nature of the beam provided by a synchrotron radiation source is of advantage over conventional focused laboratory x-ray sources for the shallow angle technique, in that the associated serious geometric aberration effects are avoided. Further, the high intensity beam provided by a synchrotron source is necessary for the relatively weak scattering from the small volume of material sampled in the shallow angle geometry; the availability of relatively hard x-rays allows a wide dynamic range (up to $\sim 18 \text{ \AA}^{-1}$).

The conventional (transmission) x-ray diffraction arrangement is modified to produce the shallow angle configuration, and both instrument configurations are shown schematically in Fig. 3. In both cases, the white beam from the synchrotron source is monochromated by a channel cut crystal and proceeds through a pair of slits

Table I. Penetration depth for x-rays incident at an angle $\alpha_i > \alpha_c$ onto diamond, silicon, and steel.

Incident angle α_i°	Penetration depth, $t \mu\text{m}$ at $\lambda = 0.5 \text{ \AA}$		
	Diamond film	Silicon wafer	Steel disk
2.0	590	125	0
1.0	295	62	0
0.5	148	31	0
0.2	59	12	0
0.1	30	6	0

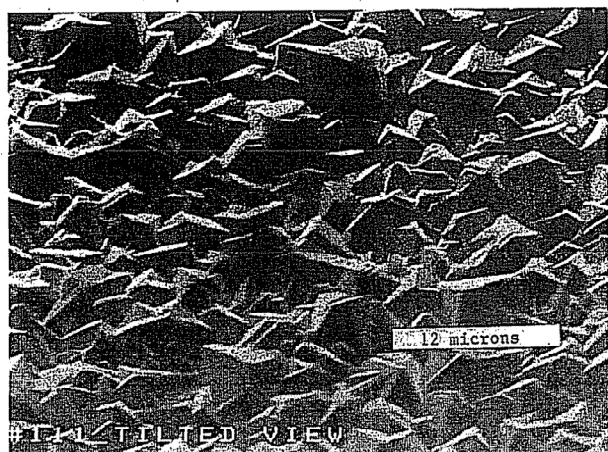


Fig. 2. Scanning electron microscopy image of CVD grown diamond film on a silicon substrate under the conditions described in the text (scale bar = 12 μ m).

which define the incident beam profile. A slit of ~ 0.8 mm by 10 mm is used for transmission work to maximize the scattered beam intensity; a narrow slit profile of 100 μ m by 10 mm is used in shallow angle work to limit contamination from the straight through beam at the lowest incident angles. For transmission diffraction, the angle θ of the sample, normal to the incident beam, is coupled to the position of the detector 2θ ; this facilitates sample corrections by producing a simple, $\cos(\theta)$ dependence in the volume of illuminated sample. The scattered radiation passes through a simple slit system to the detector where data is collected sequentially at angles $2\theta = 2^\circ$ to 130° .

For shallow angle diffraction, the sample is set at a fixed, small angle α_i to the incident x-rays. An iterative procedure of height and angle adjustment is used to define the zero-angle for the sample;^{2,3} this procedure is very important given the small angles used in data collection. It is also essential that the sample is smooth and flat: any significant irregularity in the film thickness will produce a high uncertainty in α_i and hence on the collected scattering profile. The scattered radiation passes through an arrangement of horizontal and vertical slits to the detector. A long slit package reduces the angular spread of scattered radiation incident on the detector and results in a resolution of $\sim 0.07^\circ$. Data is collected in the same angular

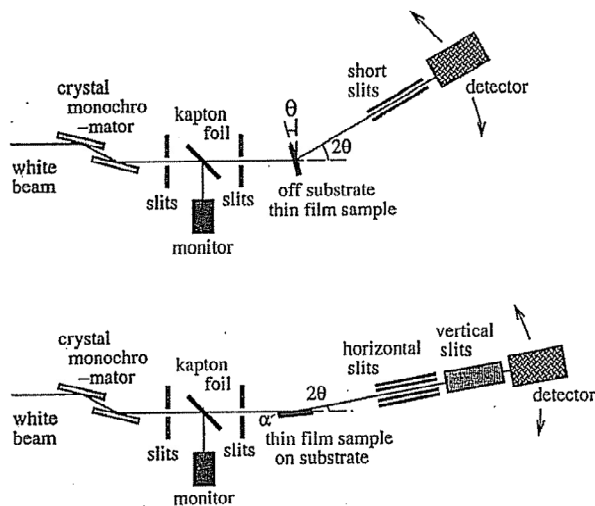


Fig. 3. (Top) The conventional transmission x-ray diffraction arrangement; (below) the arrangement for diffraction at shallow angles of incidence.

range as in the standard transmission case; this is later converted to scattering vector $|Q| = 4\pi/\lambda \sin \theta$.

Data Analysis

There are many texts detailing x-ray diffraction theory, for example Ref. 8, and this is not presented here.

Basic data reduction for both conventional and shallow angle x-ray diffraction can be carried out in a similar manner, *i.e.*, corrections are made for detector dead time, changes in incident beam current and beam polarization effects.⁹ A further correction is needed in the shallow angle geometry to account for the fact that the x-ray beam collected at the detector is actually scattered from the refracted beam in the sample; this produces a small shift in the measured scattering angle 2θ .³

More sample-specific corrections, such as sample absorption and conversion to absolute units, are not included in the reduction procedure for the shallow angle technique; both are complicated by unknown factors in the sample geometry, which means it is difficult to measure the actual penetration depth into the sample and/or substrate and therefore the contribution to absorption effects from each. This situation could be clarified if the films were thick enough to ensure that the incident x-rays did not penetrate the substrate; this would, however, limit the usefulness of the technique as a probe sensitive to different depths of the thin film, such as surface or interlayer effects. Reduction of the incident angle or increasing the incident x-ray wavelength reduces the need for very thick samples and alleviates this problem somewhat; however, increasing λ decreases the Q range and therefore the real-space resolution. Subtraction of the background scattering in the shallow angle geometry can also be problematic, as it is very difficult to measure; however, for scattering from crystalline materials, where the bulk of the scattering is concentrated in sharp Bragg reflections, this does not reduce the amount of information obtainable from the data. The lack of such well-defined corrections means that the technique still needs development, particularly for studying amorphous materials, and limits the quantitative nature of shallow angle measurements: the method is, however, useful for showing qualitative changes within a series of films or in a single film following postdeposition treatment (*e.g.*, annealing).

Results and Discussion

Diffraction data for the CVD diamond film deposited onto a silicon wafer was collected at an incident x-ray wavelength of 0.5 \AA and at sample angles α_i of 2.0° , 1.0° , 0.5° , 0.2° , and 0.1° . Figure 4 shows a comparison of the corrected shallow angle scattering profiles, with highest α_i uppermost; Table II gives the positions of the major peaks in each data set. It is immediately clear that the sharp peaks associated with the silicon substrate, such as those

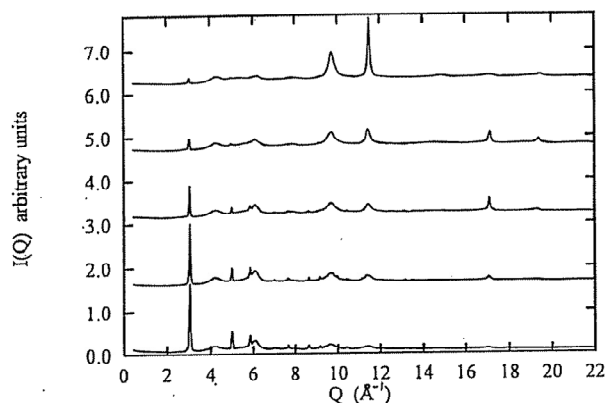


Fig. 4. Scattering from the CVD diamond thin film sample deposited on silicon at a variety of incident angles, from top to bottom $\alpha_i = 2.0^\circ$, 1.0° , 0.5° , 0.2° , and 0.1° .

Table II. Major peak positions in the shallow angle data of CVD diamond deposited on silicon for various α_i , with peak assignments: D, diamond; Si, silicon; Si-C, silicon-carbon.

α_i°	Major peak positions in $Q \pm 0.02$ (\AA^{-1})									
2.0	3.05	4.32			6.15		7.84			8.60
1.0	3.05	4.23	4.98	5.83	6.11		7.66			
0.5	3.05	4.23	4.98		6.10	6.95	7.66			8.64
0.2	3.02	4.23	4.98	5.83	6.06	7.05	7.66			8.64
0.1	3.05	4.23	4.98	5.83	6.06	7.00	7.67	8.04		8.64
Assignment	D	Si	D	D	Si	D	D	D		D

α_i°	Major peak positions in $Q \pm 0.02$ (\AA^{-1})									
2.0		9.72				11.56	14.92	17.11		19.45
1.0		9.12	9.72			11.46	14.94	17.10		19.40
0.5		9.16	9.63		10.43	11.42	14.52	17.10		19.35
0.2		9.16	9.67	9.96	10.43	11.42		17.05		
0.1		9.16	9.63	9.96	10.43	11.13	11.46	17.00		
Assignment	D	Si	D	D	D	Si	Si	Si/Si-C	Si/Si-C	

at ~ 9.7 and ~ 11.5 \AA^{-1} , decrease rapidly when the incident angle is decreased (and therefore the penetration depth into the sample/substrate falls), whereas those associated with the diamond film, e.g., the diamond {111}, {220}, and {311} reflections at 3.05, 4.98, and 5.83 \AA^{-1} , increase as α_i approaches α_c . The silicon peaks at higher Q become less sharp and other diamond peaks such as those at ~ 9 \AA^{-1} {511} appear as scattering from the thin film is isolated.

The two peaks at ~ 17.1 and ~ 19.4 \AA^{-1} do not follow this trend, in fact the peaks sharpen at a penetration depth corresponding to $\alpha_i = 1.0^\circ$ and shift to slightly shorter Q -values (larger d spacing). This may indicate that the penetration depths associated with this geometry probe a highly ordered Si-C interfacial layer between the silicon and diamond. (Silicon:carbon interfacial regions have been observed by many workers using other probes/methods; see for example Ref. 9 and references therein.) The peak at ~ 6.1 \AA^{-1} , tentatively assigned to silicon, also exhibits some unusual characteristics: it is broad at higher values of α_i , but appears to become sharper as the incident angle is decreased, suggesting it is a feature associated with the film, not the substrate. However, its presence in the $\alpha_i = 2.0^\circ$ scan, which has little contribution from the diamond film, indicates the contrary: it may be that the peak appears more intense due to the sharpening of the diamond peak at 5.83 \AA^{-1} on its lower Q side. Alternatively, this peak could be near-surface graphitic material which would exhibit diffracted intensity in the same region (however, lower order graphitic reflections are not visible which casts some doubt on this speculation).

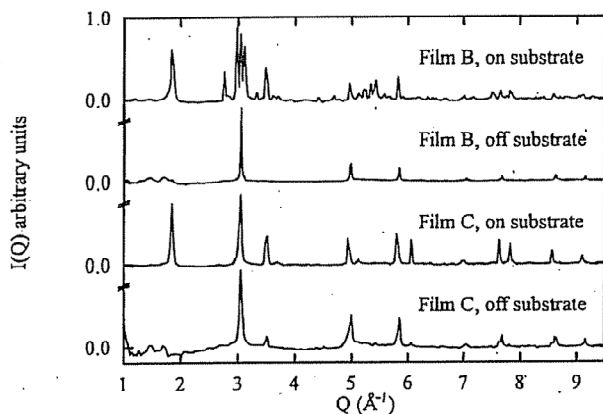


Fig. 5. Scattering from the CVD diamond on steel showing a comparison of the two films and the transmission and shallow angle diffraction results.

Table III. Prominent peak positions in the shallow angle data of film B and C in the range 2.50 to 4.50 \AA^{-1} , with peak assignments: D, diamond; G, graphite; Fe, iron; Ni, nickel; ?, unknown.

Film	Mode	Peaks in Q -range 2.50 to 4.50 \AA^{-1} in $Q \pm 0.02$ (\AA^{-1})									
B	Shallow	2.76	2.85	2.98	3.05	3.10	3.32	3.49	3.61	3.70	4.41
C	Shallow				3.06			3.50		3.70	
Assignment		?	?	G	D	Fe	?	G	Ni	G	Fe

The CVD diamond films on steel disks were examined using an x-ray wavelength of 0.7 \AA , slightly higher than for film A. A higher incident wavelength means that the penetration depth for each α_i is decreased, but the available Q range measurable is reduced. For materials exhibiting Bragg scattering this is convenient as structural information is concentrated at lower Q values, with the advantage that the need for thicker films is lessened. Data was collected at incident angles of 0.05°, 0.1°, and 2.0°; however, it was found that at all incident angles a contribution from the substrate was visible to some extent. There are several possible reasons for this: the film could be thinner than estimated so that incident x-rays always penetrate through to the substrate below; there could be cracks or irregularities in the film such that the steel is effectively more visible; or the surface of the steel could be very rough so that the interface layer is wide and hence effectively near the surface. Since the surface of the steel disk was prepared by shock implantation^{9,10} to enhance nucleation, the surface will be rough; the latter option is therefore considered the most likely. Further work is underway to study CVD diamond on polished steel.

Figure 5 shows scattering from films B and C at a shallow angle of 0.05° and incident x-ray wavelength of 0.7 \AA ; compared with transmission diffraction measurements of identical films removed from the substrate. Transmission diffraction will give information on the averaged structure throughout the film, i.e., it is not possible to distinguish the structure in the bulk of the film and in the interface or surface regions. The transmission measurements are therefore expected to contain information predominantly on the bulk of the sample, whereas shallow angle measurements will be sensitive to structural information at a penetration depth determined by the angle of incidence: this could be associated with the film, interface region or substrate, or most likely as a weighted mean of these components.

The scattering from film B, off substrate, reveals clear Bragg peaks at positions and reflections corresponding to a diamond arrangement: 3.06 {111}, 4.98 {220}, 5.86 {311}, 7.04 {400}, 7.70 {331}, 8.62 {422}, 9.19 {511}, 9.97 {440}, and 10.41 \AA^{-1} {531}; there are no other strong Bragg peaks. Similarly, for film C, off substrate, the significant peaks result from diamond reflections, although an additional peak is clear at 3.49 \AA^{-1} , thought to result from a graphite {102} reflection. This suggests that there is indeed a small amount of graphitic carbon within the sample. The shallow angle results for film B, however, clearly show many strong nondiamond peaks, indicating that even at $\alpha_i = 0.05^\circ$ the x-rays have penetrated to the steel substrate. Table III shows the major peak positions in the region $Q = 2.5$ to 4.5 \AA^{-1} , together with tentative assignments where possible. Strong Bragg peaks from graphite, iron, and nickel are visible, as are several more sharp peaks originating from other, less easily defined, constituents of the steel disk. In particular, two additional strong peaks are present either side of the diamond {111} peak at 3.06 \AA^{-1} , the graphite {100} peak at 2.98 \AA^{-1} , and the iron {110} peak at 3.10 \AA^{-1} . In contrast, the shallow angle diffraction pattern from film C shows very little contamination from the steel substrate, the visible Bragg peaks result from the expected diamond structure but also graphitic interlayer distances. The latter peaks are probably due to graphitic structure in the film, perhaps in the interface or surface

region. It is important to note, however, that these results are not consistent with there being a significant proportion of iron carbide present in the film.

Conclusion

The novel shallow angle technique has been successfully used to produce a preliminary structural study of a diamond thin film deposited onto a silicon wafer in its as-deposited state. While the thin film structure has not been completely isolated at $\alpha_1 = 0.1^\circ$, the reduction in scattering from the silicon substrate is significant; the sample scattering could be isolated further by reducing the angle of incidence to lower angles (and improving the resolution of the detector). The data presented here were collected at x-ray wavelengths of 0.5 Å; increasing this would increase the attenuation coefficient for the film thereby reducing the penetration depth and achieving the same effect, albeit at the expense of a reduction in the Q range. For crystalline samples this would be the favorable option as structural identification can be achieved from a more limited range of reciprocal space data.

The comparison of the CVD diamond films deposited onto steel disks examined in their as-deposited state by shallow angle diffraction, and off substrate by conventional transmission x-ray diffraction, revealed that the shallow angle data showed contributions from the scattering from the steel; this may be due, in part, to the steel being initially prepared by the shock implantation of diamond as a base for the CVD process. Work is underway to study CVD diamond films on finely polished steel substrates, which should help solve these problems. The availability of high quality shallow angle data for these films, together with the transmission data, would be useful in helping to solve some of the correction procedures which are at

present limiting the quantitative nature of the technique, and thereby allow the method's full use in the diffraction study of thin film structures.

Acknowledgments

We are grateful to G. Bushnell-Wye for his assistance in the early stages of the x-ray method used. We acknowledge the financial support of the SERC (now EPSRC) and the use of the SRS at Daresbury for the diffraction measurements.

Manuscript submitted June 6, 1995; revised manuscript received Nov. 27, 1995.

REFERENCES

1. W. P. G. Lim and C. Ortiz, *J. Mater. Res.*, **2**, 471 (1987).
2. T. M. Burke, D. W. Huxley, R. J. Newport, and R. Cernik, *Rev. Sci. Instrum.*, **63**, 1150 (1992).
3. T. M. Burke, Ph.D. Thesis, University of Kent (1994).
4. *Synthetic Diamond: Emerging CVD Science and Technology*, K. E. Spear and J. D. Dismukes, Editors, John Wiley & Sons, Inc., New York (1994).
5. A. H. Lettington, in *Diamond and Diamond-Like Films and Coatings*, J. C. Angus, R. E. Clausing, L. L. Horton, and P. Koidl, Editors, Plenum Publishing, New York (1991).
6. M. G. Jubber, J. I. B. Wilson, I. C. Drummond, P. John, and D. K. Milne, *Vacuum*, **45**, 499 (1994).
7. G. H. Vineyard, *Phys. Rev. B*, **26**, 4146 (1982).
8. B. E. Warren, *X-Ray Diffraction*, Dover Publications, Inc., New York (1990).
9. P. John, C. Graham, D. K. Milne, and J. I. B. Wilson, *Diamond Rel. Mater.*, (1995).
10. P. John, I. C. Drummond, and J. I. B. Wilson, in *Proceedings of Diamond Films '95*, Barcelona, 1995; To be published in *Diam. Rel. Mater.*; also, U.K. Pat. A 9211107.9 (1992).

Reactive Ion Etching of 6H-SiC in SF₆/O₂ and CF₄/O₂ with N₂ Additive for Device Fabrication

R. Wolf and R. Helbig

Institut für Angewandte Physik, Universität Erlangen-Nürnberg, D-91058 Erlangen, Germany

ABSTRACT

Reactive ion etching (RIE) of 6H-SiC in fluorinated plasmas, such as CF₄ and SF₆ with oxygen and nitrogen addition, has been investigated. Extreme anisotropic mesa structures necessary for p-n diodes were fabricated. The influence of oxygen and nitrogen gas flow on etching rates and selectivity to Si was examined. For the pure CF₄ system etching rates were very small, whereas in pure SF₆ the results were relatively high (probably due to the higher reactivity of S). As expected the etching rates increase drastically in CF₄ with the addition of O₂; in SF₆ the behavior is more complicated. The addition of N₂ to CF₄/O₂ plasmas largely enhances the etching rate, whereas in SF₆/O₂ the etching rates decrease with N₂ addition due to formation of complex molecules under F participation. A selectivity higher than unity for the SiC:Si system was observed for oxygen flows higher than 25 sccm (CF₄/N₂) and 60 sccm (SF₆/N₂). The etching rate of SiC depends linearly on applied RF power in CF₄; nitrogen addition enhances etching by a factor of approximately 1.4. In SF₆ nitrogen has only minor effects on etching rates but for applied RF powers higher than 200 W the etching rates increase strongly, indicating a change in plasma chemistry more suitable for SiC etching. Atomic force microscopy proved the usefulness of RIE for surface preparation, like polishing damage removal and smoothing for oxidation or epitaxy. Anisotropic etching behavior of the C- and Si-face of SiC samples under certain plasma conditions give way to the formulation of a new three-step etching model for RIE of SiC.

Introduction

Precise control of etching rates and etch profiles is necessary for future commercial device fabrication using SiC. Due to the chemical properties of SiC, etching in chemical solutions or molten salts leads to unsatisfactory results,^{1,2} thus leaving reactive ion etching (RIE) as the only practicable means of controlled pattern transfer in SiC processing. RIE of SiC has been reported using various fluorinated gases, on both α - and β -SiC.³⁻⁷

Typically RIE is used for pattern etching of mesa structures for fabrication of p-n diodes due to the lack of sufficiently mastered planar techniques.^{8,9} RIE also allows easy surface preparation for epitaxy and oxidation leading to smooth and homogenous structures. Occurring problems like surface roughing or micromasking can be avoided using additives, changing plasma parameters or electrode configuration.¹⁰

In this work RIE of 6H-SiC in CF₄/O₂ and SF₆/O₂ with addition of N₂ was performed and etching rates, surface